AD-A099 805 NATIONAL AERONAUTICS AND SPACE ADMINISTRATION HAMPTO--ETC F/G 11/4
EFFECTS OF STATIC TENSILE LOAD ON THE THERMAL EXPANSION OF GR/P--ETC(U)
JUN 81 G L FARLEY
UNCLASSIFIED NASA-L-14012 NASA-TP-1867 NL

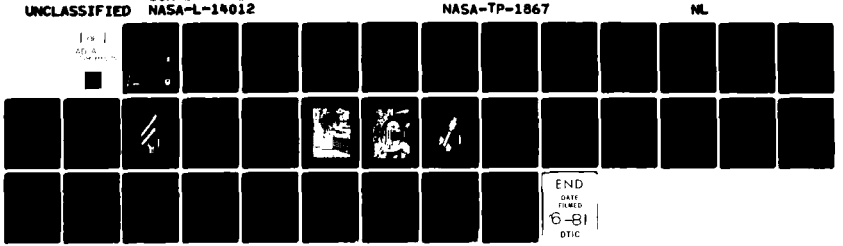

END
DATE FILMED
6-81
DTIC

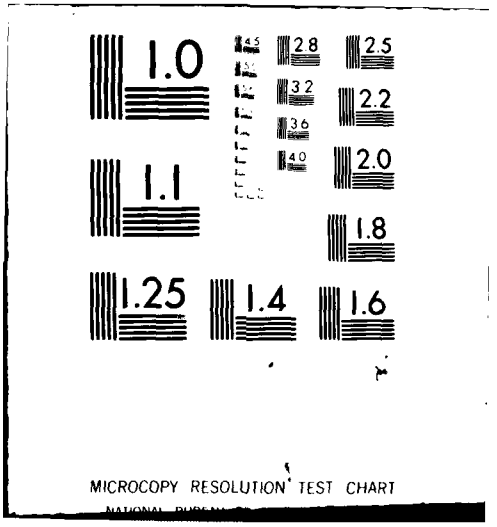
1.0
1.1
1.25
1.4
1.6
1.8
2.0
2.2
2.5
2.8
3.2
3.6
4.0
MICROCOPY RESOLUTION TEST CHART

NASA
Technical Paper 1967

AVRADCOM
Technical Report 81-B-2

LEVEL II

AD A099805

Effects of Static Tensile Load on the Thermal Expansion of Gr/PI Composite Material

DTIC
ELECTE
JUN 0 8 1981
S D
E

Gary L. Farley

JUNE 1981

DISTRIBUTION STATEMENT A
Approved for public release;
Distribution Unlimited

81 6 08 [illegible]

NASA Technical Paper 1867

USAAVRADCOM Technical Report 81-B-2

Effects of Static Tensile Load on the Thermal Expansion of Gr/PI Composite Material

Gary L. Farley
Structures Laboratory
AVRADCOM Research and Technology Laboratories
Langley Research Center
Hampton, Virginia

Accession For
NTIS GRA&I
DTIC TAB
Unannounced
Justification
By
Distribution/
Availability Codes
Dist | Avail and/or Special
A

NASA
National Aeronautics and Space Administration
Scientific and Technical Information Branch
1981

SUMMARY

The effect of static tensile load on the thermal expansion of Gr/PI composite material was measured for seven different laminate configurations. A computer program was developed which implements laminate theory in a piecewise linear fashion to predict the coupled nonlinear thermomechanical behavior.

Static tensile load significantly affected the thermal expansion characteristics of the laminates tested. This effect is attributed to a fiber-instability micromechanical behavior of the constituent materials. Analytical results correlated reasonably well with free thermal expansion tests (no load applied to the specimen). However, correlation was poor for tests with an applied load.

INTRODUCTION

Fiber-reinforced composite materials have been used extensively in aircraft secondary structure (refs. 1 and 2) during the past decade. Presently, many of the questions relating to the mechanical properties and fabrication techniques have been answered which has given the structural designer sufficient confidence for application to primary structure (refs. 3 to 5). Future designs can take advantage of the inherent characteristics of composites to tailor the structural response to meet particular design requirements (ref. 6).

Before full advantage of the tailorability of composites can be achieved, more in-depth study must be made to understand the various thermomechanical behaviors. One such phenomenon is the effect of load on the thermal expansion.

The effects of static tensile load on the coefficient of thermal expansion of mild steel and Invar were examined to a limited degree in reference 7. Resistance-type strain gages and a dead-load tensile test machine with a thermal chamber were used. A thermally calibrated material (Invar) was used to compensate for apparent thermal strain. In all tests the specimens were reported to reach a thermal and mechanical equilibrium prior to data being recorded. Using this test method, the authors reported a resolution on the order of 10^{-7} (cm/cm)/K.

A more recent study (ref. 8) was made of the effects of static compressive load on the thermal expansion of a $[\pm 45]_s$ laminate composed of Celion 6000[1] graphite fiber with PMR-15 polyimide resin. The results of that study showed that the static compressive load affected the thermal expansion of the composite material but, due to the limited number of tests and the reported quality of specimens tested, the magnitude of the effect could not be clearly established.

---

[1]Celion 6000 is a registered trademark of the Celanese Corporation.

For the study reported in reference 8, resistance-type strain gages were used to measure strains and thermocouples were used to monitor the specimen temperature. An IIT/Research Institute compression specimen was used in a thermal chamber with load applied by a displacement-controlled test machine. Compensation for apparent thermal strain was accomplished using quartz as a control material. All tests were performed using a continuous heating cycle at a constant heating rate of 83 K/hr. Data were recorded without insuring that the specimen had reached an equilibrium state.

The present study examines the thermal expansion characteristics of Celion 6000 graphite fiber with PMR-15 polyimide resin, between room temperature (RT) and 560 K. These tests were performed for free thermal expansion (no applied load) and applied static tensile load conditions. A computer program was developed which implements laminate theory in a piecewise linear fashion to predict the coupled nonlinear thermomechanical behavior. Comparison of the analytical and experimental results are made. Seven different laminates - $[0_4]$, $[90_4]$, $[\pm 30]_s$, $[\pm 45]_s$, $[0/90]_s$, and $[90/-45/0/45]_s$ - were tested. The effect of static tensile load on the thermal expansion characteristics of each laminate is compared with its free thermal expansion behavior.

The use of trade names in this publication does not constitute an endorsement, either expressed or implied, by the National Aeronautics and Space Administration.

SYMBOLS

$[A]$	laminate stiffness matrix
CTE	coefficient of thermal expansion
E_{11}, E_{22}	tangent modulus in fiber and transverse-to-fiber direction in principal material coordinate system
G_{12}	shear modulus in principal material coordinate system
$\{N\}$	vector of normal stress resultants
$[\bar{Q}]^i$	ith lamina constitutive matrix oriented in laminate reference frame
RT	room temperature
T	temperature
ΔT	temperature increment
t^i	thickness of ith lamina
α_{11}, α_{22}	coefficients of thermal expansion in fiber and transverse-to-fiber direction in principal material coordinate system

$\{\alpha_x\}^i$	ith lamina coefficient of thermal expansion oriented in laminate reference frame
$\{\bar{\alpha}\}$	vector of laminate coefficients of thermal expansion
ε	strain
$\{\varepsilon\}$	vector of midplane strains
ε^{APP}	apparent thermal strain of gage
ε^T	thermal strain
ε_{11}^T	thermal strain in fiber direction
ε_{22}^T	thermal strain transverse to fiber
ν_{12}	Poisson's ratio in principal material coordinate system
σ	stress
σ^{ULT}	ultimate stress
τ_{12}	shear stress in principal material coordinate system

TEST SPECIMENS AND INSTRUMENTATION

The experimental test matrix for this program is presented in table 1. Seven different laminate configurations - $[0_4]$, $[90_4]$, $[\pm30]_S$, $[\pm45]_S$, $[\pm60]_S$, $[0/90]_S$, and $[90/-45/0/45]_S$ - were tested with varying applied load conditions over a temperature range from RT to 560 K. All specimens were kept in a laboratory environment prior to testing. Based upon previous tests, moisture absorption was not considered a significant problem. The fiber volume fraction for all laminates tested was between 0.44 and 0.47. Nominal specimen dimensions are 20.3 cm long by 2.5 cm wide with a 12.7-cm gage length as depicted in figure 1. Load introduction tabs were fabricated with Gr/PI identical to the test laminate to minimize any mismatch in thermal expansion. High-temperature strain gages (BLH FSM-12-35-SO), placed axially back-to-back and transversely, were bonded to all specimens using a polyimide adhesive (BLH PLD-700). The effects of gage transverse sensitivity were examined and found not to appreciably affect the measurement of the thermal expansion behavior of the laminates tested.

The resistance-type foil strain gages used in this study are capable of operating in excess of 560 K. Electrical wires about 1.5 m long were silver soldered to the strain gages. For all tests, individual gages were connected to a full bridge using a three-wire system.

A digital thermometer with type E thermocouple wire (Nickle chromium/constantan) attached to the specimen was used to monitor the temperature. The temperature was displayed in increments of $0.1^{\circ}F$ to assist in determining when

thermal equilibrium was reached. Wire thermocouples were selected rather than other devices because of their greater versatility and temperature sensitivity and because they are not affected by coupled thermomechanical behavior of the test specimen.

The calibrated specimen, as shown in figure 1, used to compute the apparent thermal strain was made of titanium silicate. The specimen and detailed data on its expansion characteristics were supplied by the Corning Glass Works. The coefficient of thermal expansion (CTE) for titanium silicate is presented in figure 2. For all calculations in this study the mean value was used. Six strain gages, three back-to-back, were adhesively bonded to the titanium silicate specimen. Tests were conducted under the same thermal conditions as the composite specimens except for the application of load. The apparent thermal strain ϵ^{APP} of the gage, as depicted in figure 3, was computed by taking the difference of the measured and calibrated responses of the titanium silicate.

A titanium coupon specimen (fig. 1) 26.7 cm long and 2.5 cm wide was used to determine the applicability of the thermal expansion test method. Strain gages were oriented axially, transversely, and at 45° relative to the longitudinal axis of the specimen. Results from this test are discussed later.

TEST PROCEDURE

The test procedure consists of the following sequential steps:

(1) Align and attach test fixture to specimen.

(2) Install fixture and specimen inside furnace to creep-frame load train and connect all instrumentation.

(3) Apply static load.

(4) Balance gages and record room-temperature strain readings.

(5) Adjust set point temperature approximately 28 K above previous set point temperature.

(6) Thermally condition specimen until equilibrium is reached (approximately 15 to 40 min).

(7) Record specimen temperature and strain.

(8) If specimen temperature is below 560 K, repeat steps (5) to (7).

(9) Reduce temperature to approximately 450 K, allow specimen to reach equilibrium and record temperature and strain. (Step (9) is performed only for those tests where load was applied to the specimen for determining whether creep or plasticity occurred during the test.)

The static tensile load was applied to the specimen through a mechanical advantage in a dead-load creep frame as depicted in figures 4 and 5. Specimen

grips and alignment apparatus, illustrated in figure 6, were used to introduce a uniform tensile load into the specimen.

The magnitude of the maximum applied load for each different laminate was limited to the lesser of the load necessary to produce a strain of 0.004 at 589 K or the load corresponding to the laminate initial nonlinear stress-strain response at 589 K. The 0.004 strain limit was employed because it corresponds to a typical composite-material design strain.

A specimen was considered to be in equilibrium at a set point when the transient response of the temperature and strain dampened out and became in phase. At equilibrium the fluctuation in temperature was on the order of ±0.2 K whereas the strain varied approximately ±3με.

An examination of the effects of heating rate on the longitudinal expansion characteristics of a $[90_4]$ Gr/PI composite laminate was performed. The effects of four heating profiles from RT to 560 K to RT, as depicted in figure 7, were examined. Three profiles had constant heating rates and the fourth a step procedure. Based upon heat conduction laws, in the limit, the lower the heating rate, the nearer an equilibrium condition is achieved. The step heating procedure (profile III) is capable of producing an equilibrium condition at each step, provided the soak time is sufficiently long.

The thermal expansion of a $[90_4]$ specimen was examined using each heating profile twice. The results shown in figure 8 correspond to only one test of each heating profile since good agreement between repetitive tests was obtained. The sharp contours of the heating profiles were not reproduced because of the thermal inertia of the test chamber and specimen. Upon examination of the thermal expansion results of the four heating profiles the following trends were obtained. A nonequilibrium condition existed for heating profiles I and II; this is evident from the reduced hysteresis between the results produced for heating profiles I, II, and IV. The step heating profile of III gave results similar to those of profile IV, depicting an equilibrium or near-equilibrium state.

Based upon these results, a step heating profile was used on all subsequent tests. This heating profile, given sufficient soak time, will result in a state of equilibrium during data recording. Equilibrium was assumed to exist when the specimen temperature and the monitored strain readings became stabilized, generally resulting in soak times between 15 and 40 min.

A free thermal expansion test of a titanium alloy (Ti-6Al-4V) specimen was performed to establish the general validity of the test method. This test was performed between room temperature and 560 K. The titanium alloy was selected for its stable thermal expansion characteristics, the magnitude of the coefficient of thermal expansion, and the availability of published data (ref. 9). The thermal strain was measured and compared with published results as depicted in figure 9. Though some discrepancies exist between the measured and published results, less than 60 με, they are within nominal differences of mechanical properties between melts of the same material. This test was repeated and yielded consistent results.

ANALYSIS

Classical laminate theory was used to compare the predicted response with the measured thermomechanical response. A computer program was written to implement laminate theory in a piecewise linear manner to predict the overall nonlinear behavior. The equation governing the laminate response to mechanical load, neglecting bending, is

$$\{N\} = [A(\varepsilon,T)]\{\varepsilon\} \tag{1}$$

where

$$[A(\varepsilon,T)] = \sum_{i=1}^{M} [\bar{Q}(\varepsilon,T)]^i t^i \tag{2}$$

The $[\bar{Q}]^i$ matrix is defined as the constitutive matrix of the ith lamina, relating to stress and strain, oriented in the laminate reference frame. The thermal expansion of the laminate is governed by

$$\{\varepsilon^T\} = \{\bar{\alpha}(\sigma,\varepsilon,T)\}\ \Delta T \tag{3}$$

The vector of coefficients of thermal expansion for the laminate $\{\bar{\alpha}\}$ is defined by

$$\{\bar{\alpha}\} = [A(\varepsilon,T)]^{-1} \sum_{i=1}^{M} \{\alpha_x(\sigma,T)\}^i\ [\bar{Q}(\varepsilon,T]^i t^i \tag{4}$$

where $\{\alpha_x\}^i$ is the CTE of the ith lamina relative to the laminate reference frame. For a derivation of equation (4) the reader is referred to references 10 and 11.

As a thermal or mechanical load is applied, in small increments, the laminate material properties are updated corresponding to the temperature and stress or strain state of each ply. Load increments on the order of 5 K and 1 percent of σ^{ULT} were found to provide converged solutions.

The residual thermal stresses and any mechanically applied load are included in the analysis prior to the thermal expansion analysis. The residual thermal stresses are modeled by starting from the stress-free temperature (560 K) and reducing the temperature to room temperature. If a mechanical load is applied, then an analogous procedure is performed. An unsymmetric [0/90] laminate was heated to 589 K to determine the stress-free temperature. The

unsymmetric laminate at room temperature is deformed due to the residual thermal stresses. When heated to 560 K the specimen became flat, thus indicating a stress-free state.

The constitutive nonlinear material properties used in the analysis, E_{11}, E_{22}, G_{12}, and ν_{12}, are functions of strain and temperature whereas ε_{11}^{T} and ε_{22}^{T} are functions of stress and temperature. The constitutive properties were determined from the data presented in figures 10 to 13.

COMPARISON OF THEORY AND EXPERIMENT

The experimental results of the effect of static tensile load on thermal expansion are presented in figures 14 to 20. When repetitive tests were performed, bars denoting the nominal scatter band are used and the curve presented is the average of all tests. Each curve is a least-squares third-order polynominal representation of the experimental data. In each test nine data recordings were made during the heating cycle at increments of approximately 28 K.

The constitutive thermal expansion properties used in the analysis portion of the study, that is, ε_{11}^{T} and ε_{22}^{T}, were developed using $[0_4]$, $[90_4]$, and $[\pm 45]_s$ laminates. The $[\pm 45]_s$ laminate subjected to axial tension was used to determine the effect of shear stress on ε_{11}^{T} and ε_{22}^{T}. The validity of these data is suspect because only a limited number of $[\pm 45]_s$ specimens were available for testing and the resulting thermal expansion trends above 500 K were not expected.

A static tensile stress produced a significant effect on the longitudinal thermal expansion of the $[0_4]$ laminate as depicted in figure 14. For the free thermal expansion tests a small strain scatter band on the order of 0.0001 resulted, whereas for the cases where load was applied the maximum scatter band was on the order of 0.0004. The thermal expansion curves presented in figure 14 illustrate a characteristic "hump" between temperatures of 420 K and 500 K. The location of the hump shifts to lower temperatures with increasing applied load. This phenomenon may be attributed to the compressive residual thermal stresses in the fibers as a result of the differences in the coefficients of thermal expansion between fiber and matrix.

Although explicit evidence cannot be provided, one hypothesis of the hump phenomenon is as follows: During the cool-down phase of the cure cycle, the mismatch in thermal expansion between fiber and matrix produces a compressive residual stress state in the fibers. These compressive stresses increase until a local fiber instability occurs which alters the apparent stiffness of the laminate and results in a hump in the thermal strain curve. This hypothesis is consistent with the results of fiber microbuckling studies reported in references 12 and 13.

The free thermal expansion test is the reverse process of the cool-down procedure. As the specimen is heated, the fibers tend to be straightened by the expansion of the matrix material. Once the fibers become straightened the matrix contributions are negligible and the overall expansion characteristics are representative of the fiber. For the case where a static load is applied to a specimen, the load tends to partially straighten the fibers. Upon heating the specimen, the hump occurs at a lower temperature because the fibers have been partially straightened by the applied load.

As depicted in figure 15 the transverse thermal expansion characteristics were investigated using a unidirectional laminate with fibers oriented at 90° to the direction of the applied load. Load apparently had a lesser effect on the expansion characteristics than was the case in the $[0_4]$ laminates. One important feature was noticed in that once load was applied to the specimen the magnitude of the load had little effect on the thermal expansion characteristics of the laminate.

Based upon the results depicted in figure 16 the effects of shear stress τ_{12} on the longitudinal thermal expansion, in the fiber direction, was found to be negligible up to 500 K. At temperatures above 500 K plasticity effects contributed to the measured expansion of the laminate. Due to a limited number of specimens, repetitive tests were not performed; neither was the applied load reapplied at a lower level. The validity of the $[\pm 45]_s$ laminate thermal expansion characteristics is suspected in light of the previously mentioned plasticity effects and results from the $[0/90]_s$ and $[90/-45/0/45]_s$ laminates that are discussed herein. Further discussion of the effects of shear stress on α_{11} is provided subsequently.

As shown in figure 17, tensile load produced a significant effect on the thermal expansion of the $[\pm 30]_s$ laminate. The experimental strain scatter was less than 0.0002, for specimens tested with and without applied load. The magnitude of the thermal expansion and the overall shape of the thermal strain curves for the $[\pm 30]_s$ laminate are similar to those for the $[0_4]$ laminate. The general shape of the thermal expansion curves was predictable although the agreement between experiment and analysis was inadequate. The measured thermal expansion of the laminate under load is greater than that of the unloaded laminate. The calculations depict the opposite trend, which could be a result of the effects of shear stress on α_{11} and α_{22}. In this analysis the effects of shear stress α_{11} and α_{22} have been neglected.

As depicted in figure 18 an applied load produced a moderate effect, about 20 percent, on the thermal expansion characteristics of a $[\pm 60]_s$ laminate. At temperatures below 400 K the effect of an applied load was less than 2 percent, whereas above 400 K the difference increased to 20 percent at 500 K. The measured free thermal expansion was greater than the expansion measured under applied load. This behavior was similar to that exhibited by the $[90_4]$ laminate. Both of these laminates have matrix-dominant responses with minimal shear interaction. At temperatures below 400 K good agreement, less than 2 percent difference, between the experiment and analysis was obtained. At higher temperatures the measured free thermal expansion curve was not predictable.

Cross-ply $[0/90]_s$ and quasi-isotropic $[90/-45/0/45]_s$ laminates were tested with and without an applied load. Both laminates tested demonstrated that a static load had a significant effect on their thermal expansion behavior as illustrated in figures 19 and 20. The overall thermal expansion of these laminates is similar to that of other fiber-dominant laminates, such as the $[0_4]$ and $[\pm30]_s$ laminates. The cross-ply and quasi-isotropic laminates strain-temperature curves have a characteristics hump similar to the $[0_4]$ and $[\pm30]_s$ laminates although the hump occurs at a higher temperature for the cross-ply and quasi-isotropic laminates. This difference is suspected to be a result of the matrix-dominant response of the 90^o and 45^o plies. These matrix-dominant plies reduce the percent of 0^o plies which in effect reduces their contribution to the overall behavior of the laminate; hence, the characteristics of the hump are altered. Based upon the results of the $[0_4]$, $[0/90]_s$, and $[90/-45/0/45]_s$ laminates, with decreasing percent of 0^o fibers the hump shifts to the right, that is, occurs at higher temperatures.

The thermal expansion curve of the cross-ply laminate subjected to an applied load shifted below the free expansion curve analogous to the response of the $[0_4]$ laminate. The quasi-isotropic laminate produced results similar to those of the $[\pm30]_s$ laminate. This vertical shift of the thermal-strain curve is attributed to the angle plies in the $[\pm30]_s$ and quasi-isotropic laminates.

For both the cross-ply and quasi-isotropic laminates good agreement, differences of less than 10 percent, between experiment and analysis was obtained for the free thermal expansion tests. For the applied load conditions, agreement between experiment and analysis was poor. Furthermore, in the case of the quasi-isotropic laminate, the measured shift in the expansion curves due to load was the opposite of that predicted.

Based upon laminate theory the free thermal expansion of $[\pm45]_s$, $[0/90]_s$, and $[90/-45/0/45]_s$ laminates should be identical. Close agreement in measured free thermal expansion was found for the $[0/90]_s$ and $[90/-45/0/45]_s$ laminates while the $[\pm45]_s$ did not agree although the $[\pm45]_s$ and $[0/90]_s$ laminates were machined from the same panel. The measured thermal expansion of the $[\pm45]_s$ laminate is suspected to be in error and the shear stress effects on the longitudinal coefficient of thermal expansion α_{11} may be more significant than these measurements would indicate.

If shear stress has a significant effect on α_{11}, then the inclusion of angle plies in fiber-dominant laminates could affect the thermal expansion trends. An attempt was made to include the effects of shear stress τ_{12} on the longitudinal thermal expansion α_{11}. Because the data for the $[\pm45]_s$ laminate were suspect, data relating shear stress and α_{11} were generated such that when incorporated in the analysis, the thermal expansion characteristics of the $[\pm30]_s$ laminate subjected to load were predictable. The agreement between analysis and experiment for the quasi-isotropic laminate under load was improved using these data even though the analysis predicted a decrease in thermal expansion under load rather than the increase measured. Further tests to determine the effect of shear stress on α_{11} and a more sophisticated analysis are probably required to adequately model the coupled behavior in laminates with angle plies.

CONCLUSIONS

Based upon results obtained in this study the following conclusions can be drawn about the effects of applied load on the thermal expansion characteristics of Gr/PI composite laminates.

1. Static tensile load has an effect on the thermal expansion characteristics of the laminates tested. The magnitude of the effect is a function of the laminate orientation and, in general, the magnitude of the applied load.

2. For the laminates tested, the $[0_4]$ laminate was most strongly affected by the applied load. Fiber instability induced during cool down from the stress-free condition near the cure temperature may be a significant factor.

3. The test method used provided adequate resolution for depicting trends with a reasonable degree of scatter.

4. Reasonable correlation was obtained between experiment and analysis, based upon classical laminate theory, for the free thermal expansion tests. Poor correlation was obtained for the applied load tests. A formulation taking into account the coupled material behavior in a more rigorous fashion may be beneficial.

5. Shear stress τ_{12} could have a significant effect on the longitudinal thermal expansion coefficient α_{11} although the magnitude of its effect was not conclusively established. Further experimental and analytical studies are required to account for shear stress effects.

Langley Research Center
National Aeronautics and Space Administration
Hampton, VA 23665
May 1, 1981

REFERENCES

1. Stoecklin, Robert L.: 737 Graphite Composite Flight Spoiler Flight Service Evaluation. NASA CR-158933, 1978.

2. Kollmansberger, R. B.; and Rackiewicz, J. J.: Kevlar Composites in the Helicopter Environment. AIAA Paper 79-0805, Apr. 1979.

3. Vosteen, Louis F.: Composite Structures for Commercial Transport Aircraft. NASA TM-78730, 1978.

4. Mazza, L. Thomas; and Foye, R. L.: Advanced Composite Airframe Program - Preliminary Design Phase. Preprint No. 80-45, 36th Annual National Forum Proceedings, American Helicopter Soc., May 1980.

5. Lacagnina, Mark M., ed.: Lear Fans Will Be Built in Ireland. AOPA Pilot, vol. 23, no. 4, Apr. 1980, pp. 20-26.

6 Bush, Harold G.; Mikulas, Martin M., Jr.; and Heard, Walter L., Jr.: Some Design Considerations for Large Space Structures. AIAA J., vol. 16, no. 4, Apr. 1978, pp. 352-359.

7. Rosenfield, A. R.; and Averbach, B. L.: Effect of Stress on the Expansion Coefficient. J. Appl. Phys., vol. 27, no. 2, Feb. 1956, pp. 154-156.

8. Hashin, Z.; Rosen, B. W.; and Pipes, R. B.: Nonlinear Effects on Composite Laminate Thermal Expansion. NASA CR-3088, 1979.

9. Weiss, V.; and Sessler, J. G., eds.: Aerospace Structural Metals Handbook. Volume II - Non-Ferrous Alloys, ASD-TDR 63-741, Vol. II, Suppl. 2, U.S. Air Force, Mar. 1965.

10. Ashton, J. E.; Halpin, J. C.; and Petit, P. H.: Primer on Composite Materials: Analysis. Technomic Pub. Co. Inc., c.1969.

11. Jones, Robert M.: Mechanics of Composite Materials. McGraw-Hill Book Co., c.1975.

12. Rosen, B. Walter: Mechanics of Composite Strengthening. Fiber Composite Materials, American Soc. Metals, c.1965, pp. 37-75.

13. Sadowsky, M. A.; Pu, S. L.; and Hussain, M. A.: Buckling of Microfibers. J. Appl. Mech., vol. 34, ser. E, no. 4, 1967, pp. 1011-1016.

TABLE 1.- EXPERIMENTAL TEST MATRIX

Specimen	Laminate layup	Applied stress, MPa	Specimen	Laminate layup	Applied stress, MPa
1	$[0_4]$	0	14	$[90_4]$	18.2
2	$[0_4]$	0	15	$[\pm 60]_s$	0
3	$[0_4]$	287.0	16	$[\pm 60]_s$	0, 16.2
4	$[0_4]$	287.0	17	$[\pm 60]_s$	0
5	$[0_4]$	403.0	18	$[0/90]_s$	0, 294
6	$[0_4]$	403.0	19	$[0/90]_s$	0, 294
7	$[90_4]$	0	20	$[0/90]_s$	0, 294
8	$[90_4]$	0	21	$[\pm 30]_s$	0, 105
9	$[90_4]$	8.6	22	$[\pm 30]_s$	0, 105
10	$[90_4]$	8.6	23	$[90/-45/0/45]_s$	0, 158
11	$[90_4]$	13.4	24	$[90/-45/0/45]_s$	0
12	$[90_4]$	13.4	25	$[90/-45/0/45]_s$	158
13	$[90_4]$	18.2	26	$[\pm 45]_s$	0, 9.9

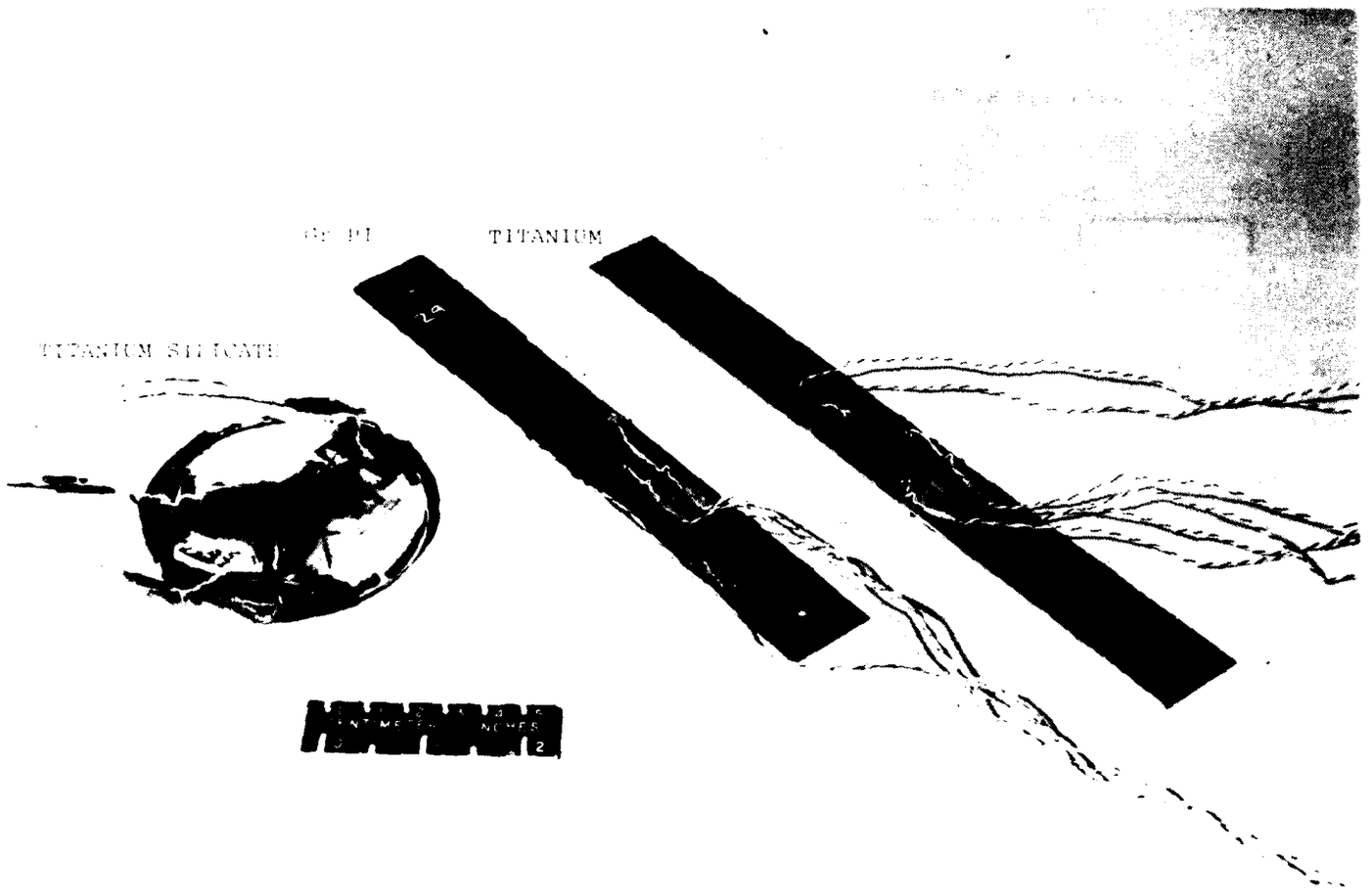

L-79-4915.1

Figure 1.- Test specimens.

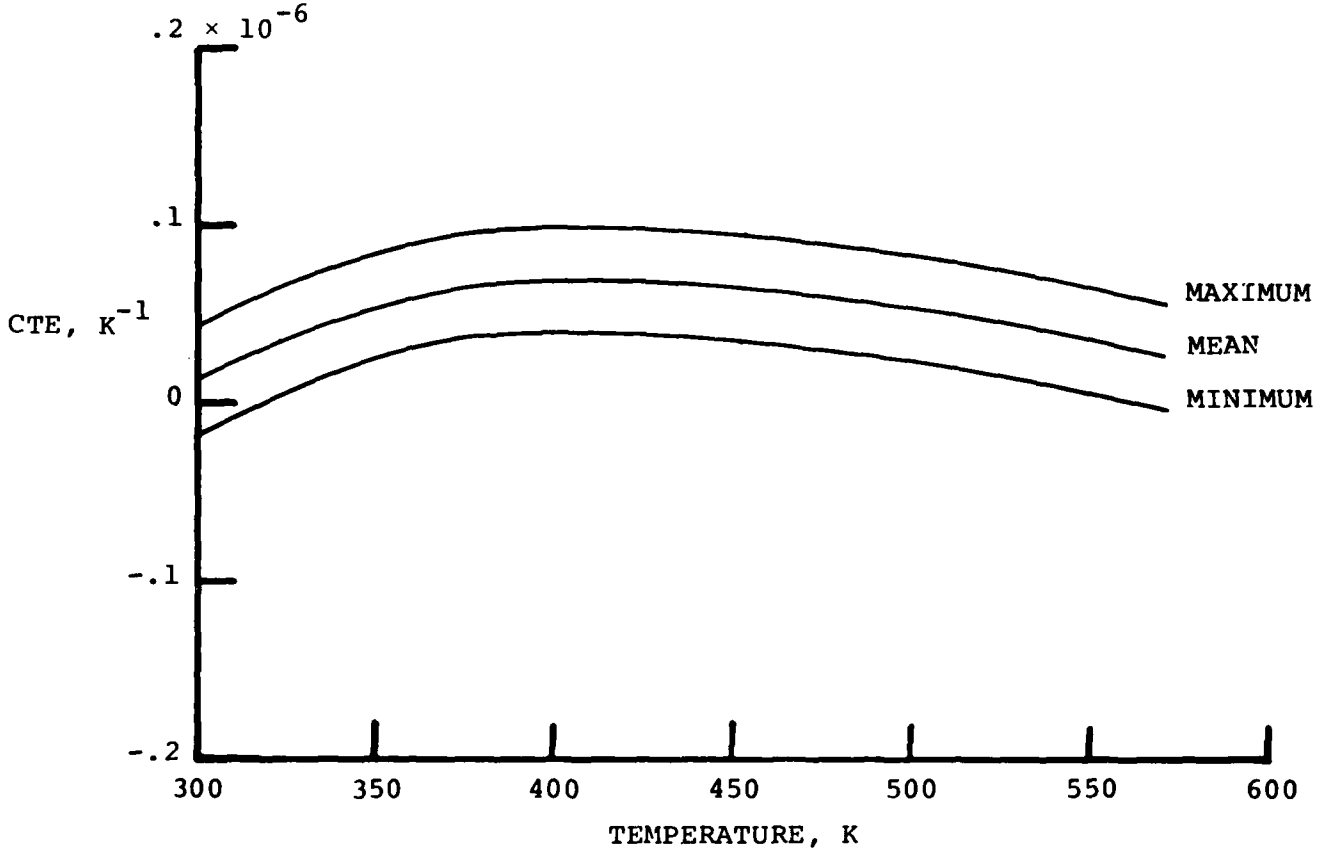

Figure 2.- Coefficient of thermal expansion of titanium silicate.

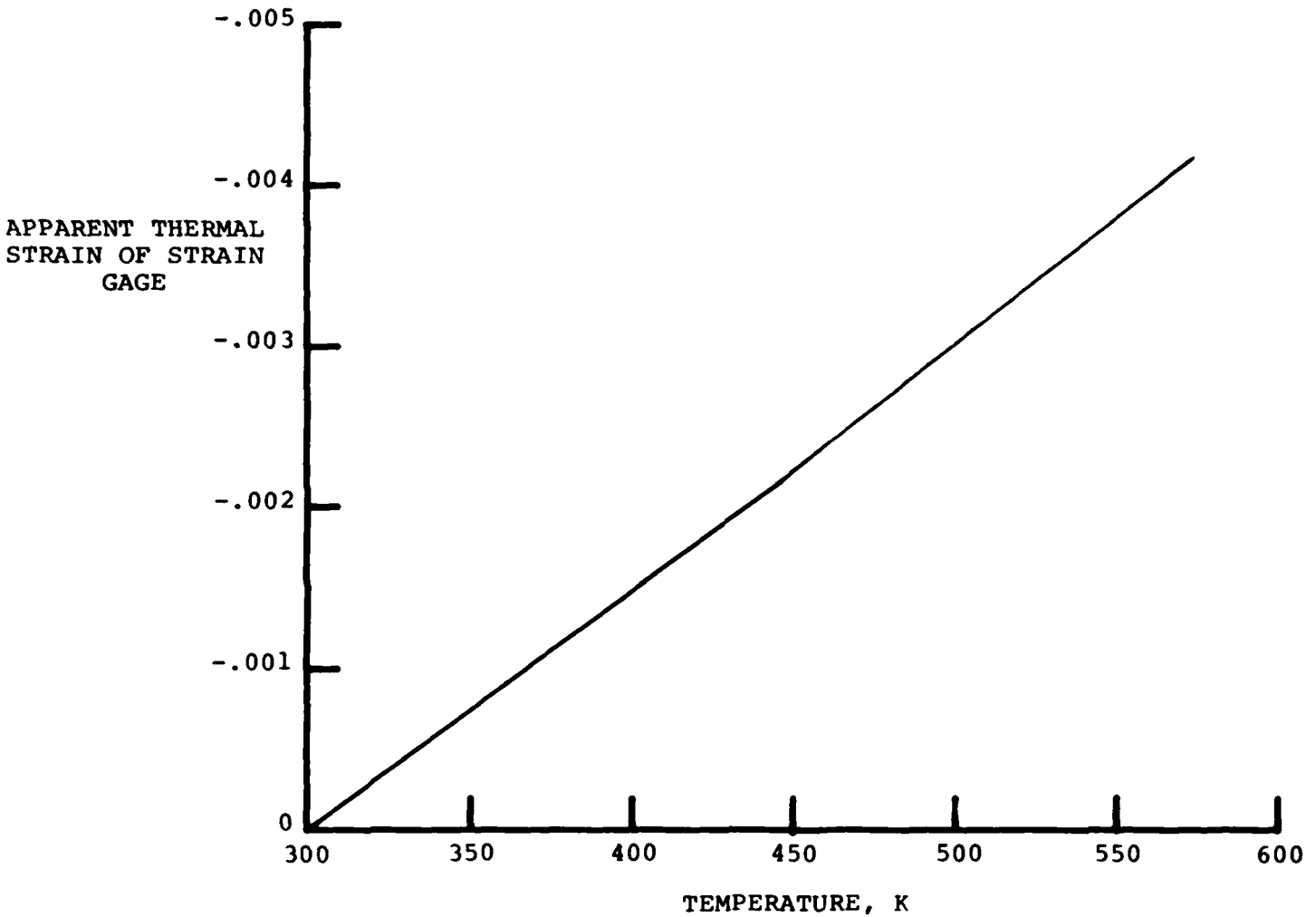

Figure 3.- Apparent thermal strain of strain gage.

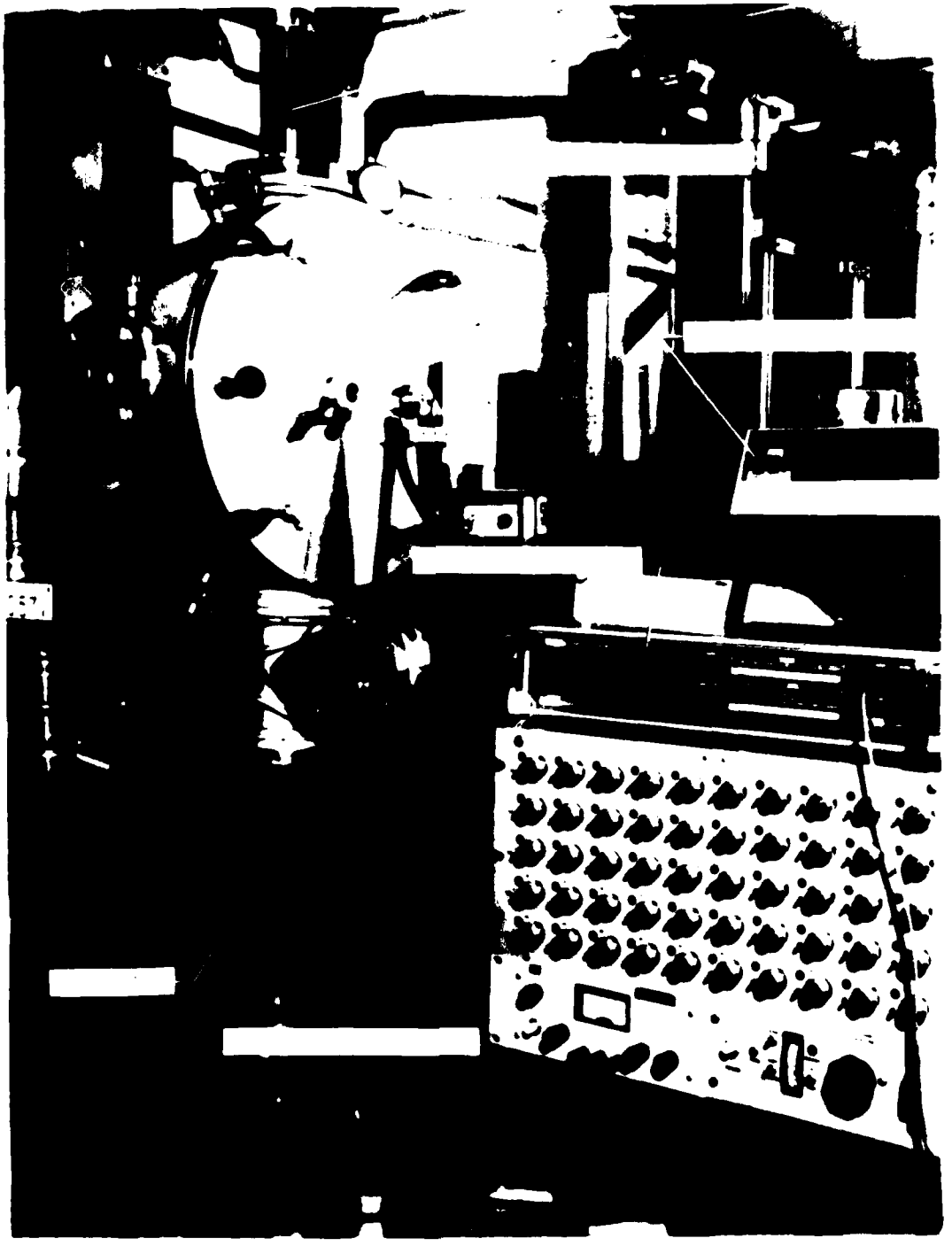

L-79-4917.1

Figure 4.- Test apparatus.

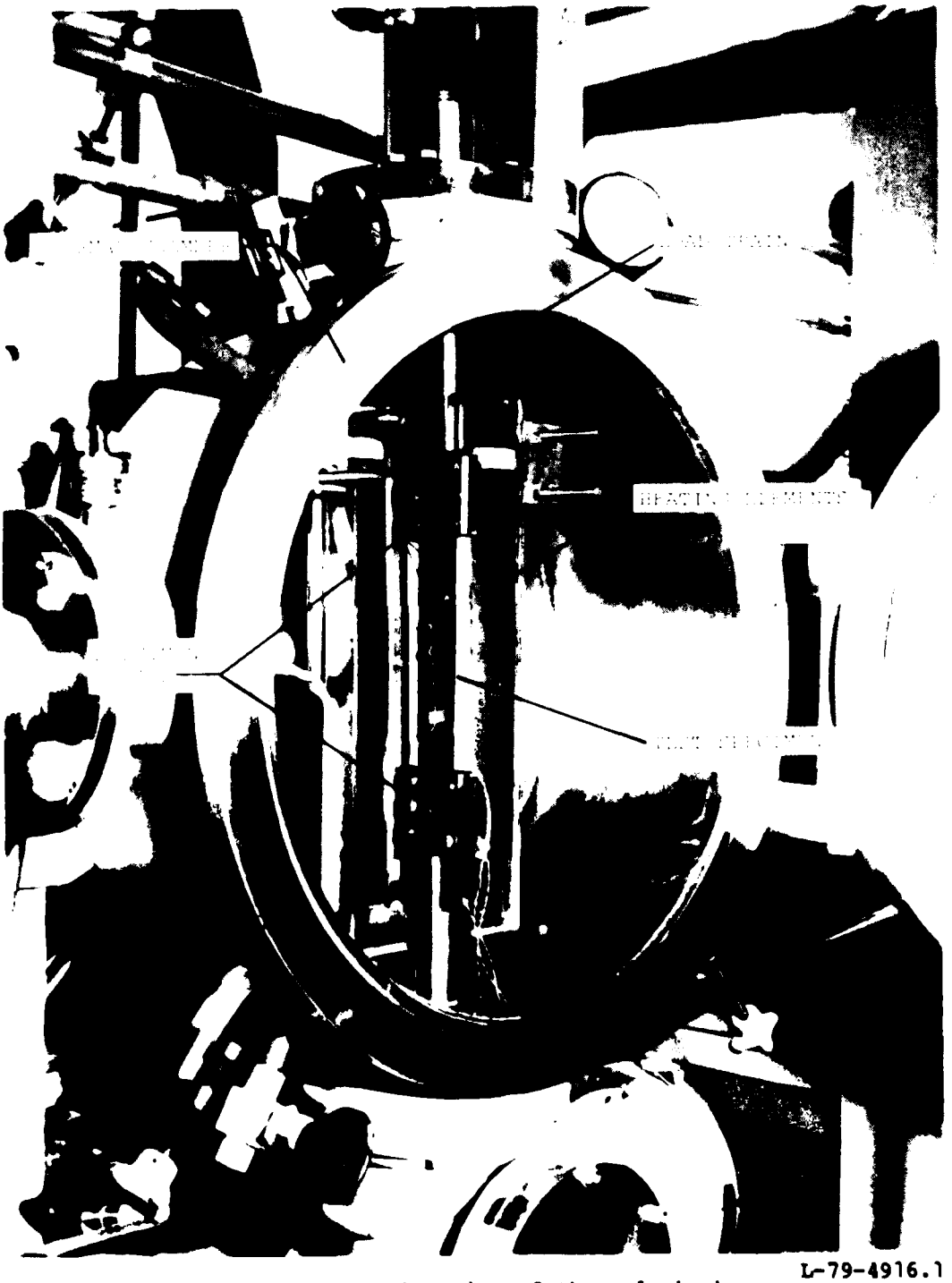

L-79-4916.1

Figure 5.- Interior view of thermal chamber.

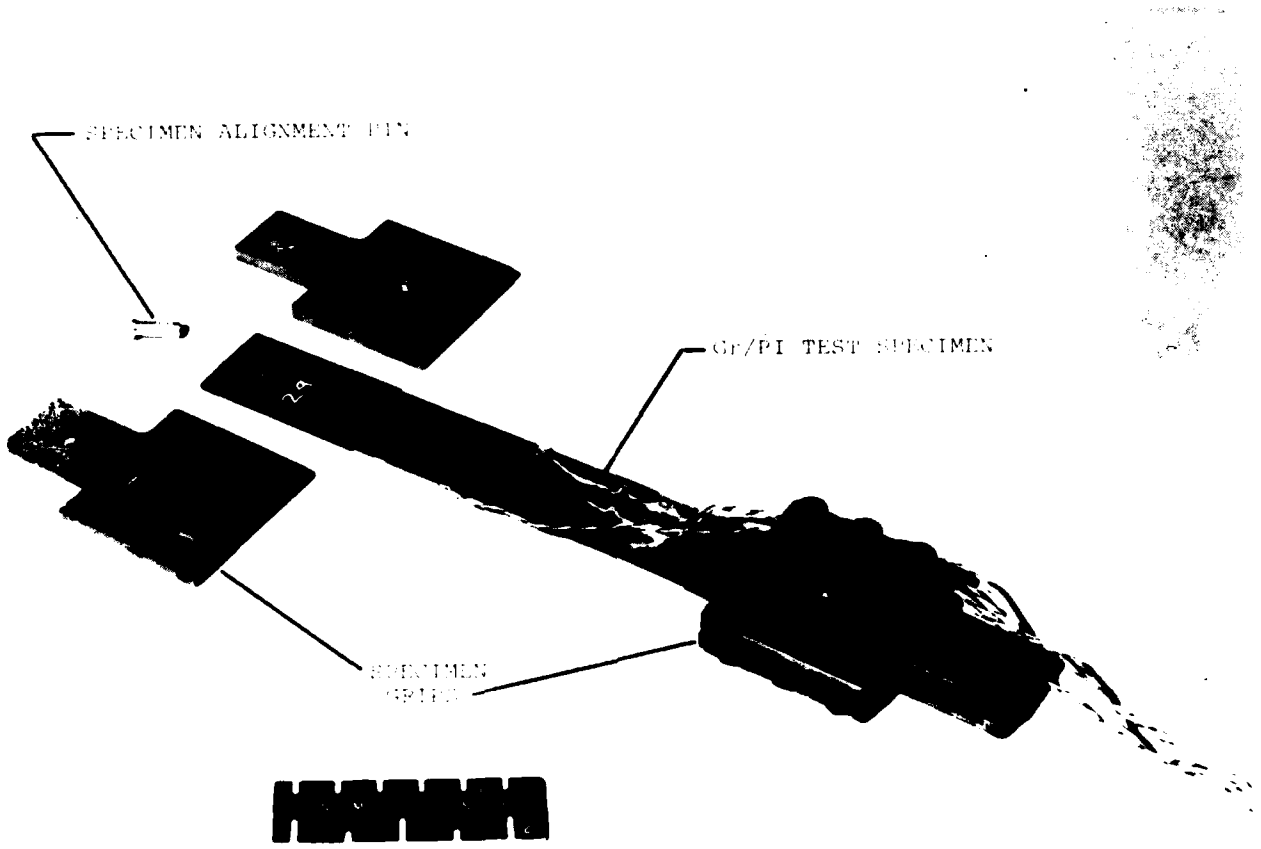

L-79-4914.1

Figure 6.- Typical test specimen and bolted load introduction fixture.

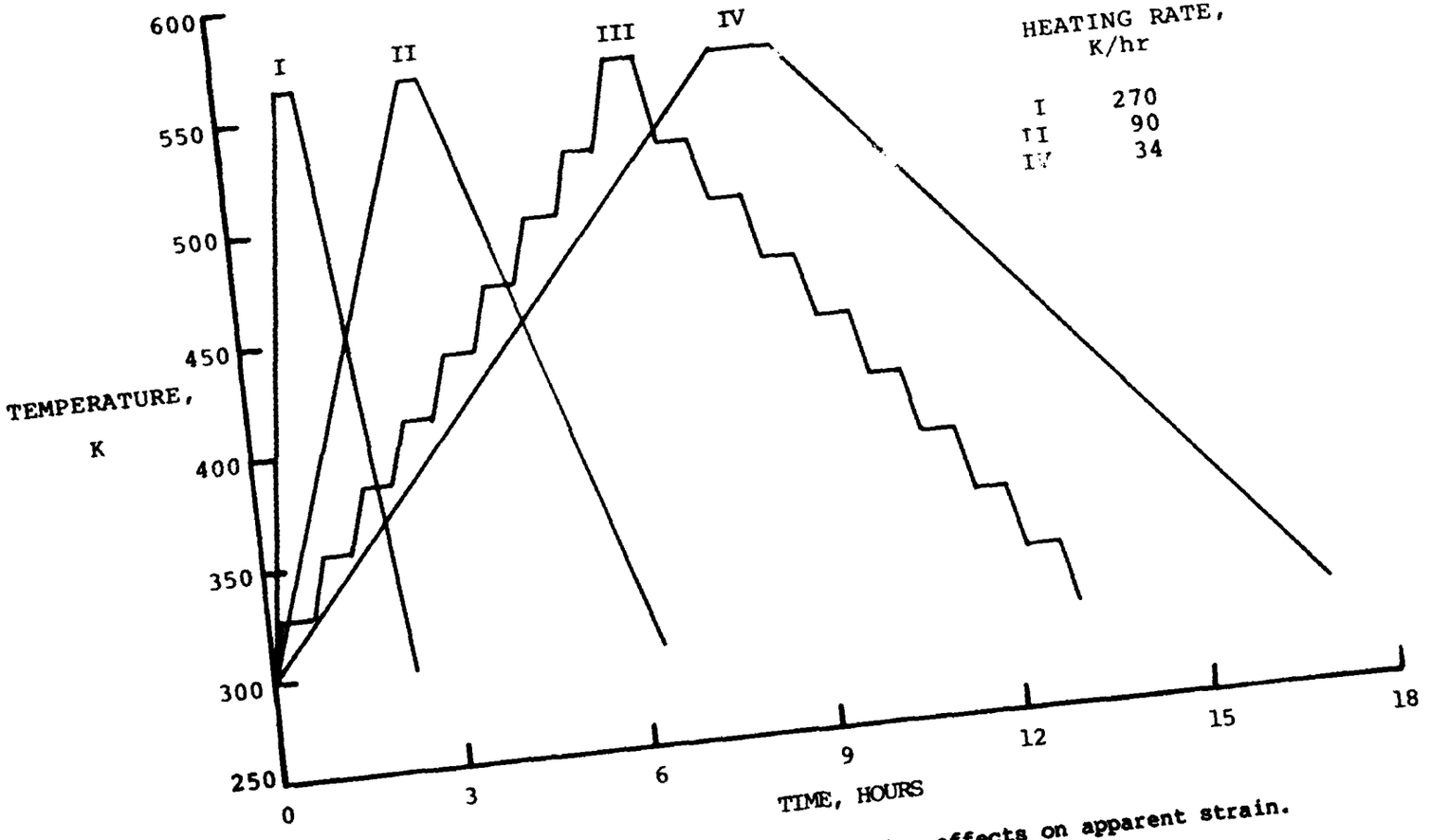

Figure 7.- Heating profiles investigated to determine effects on apparent strain.

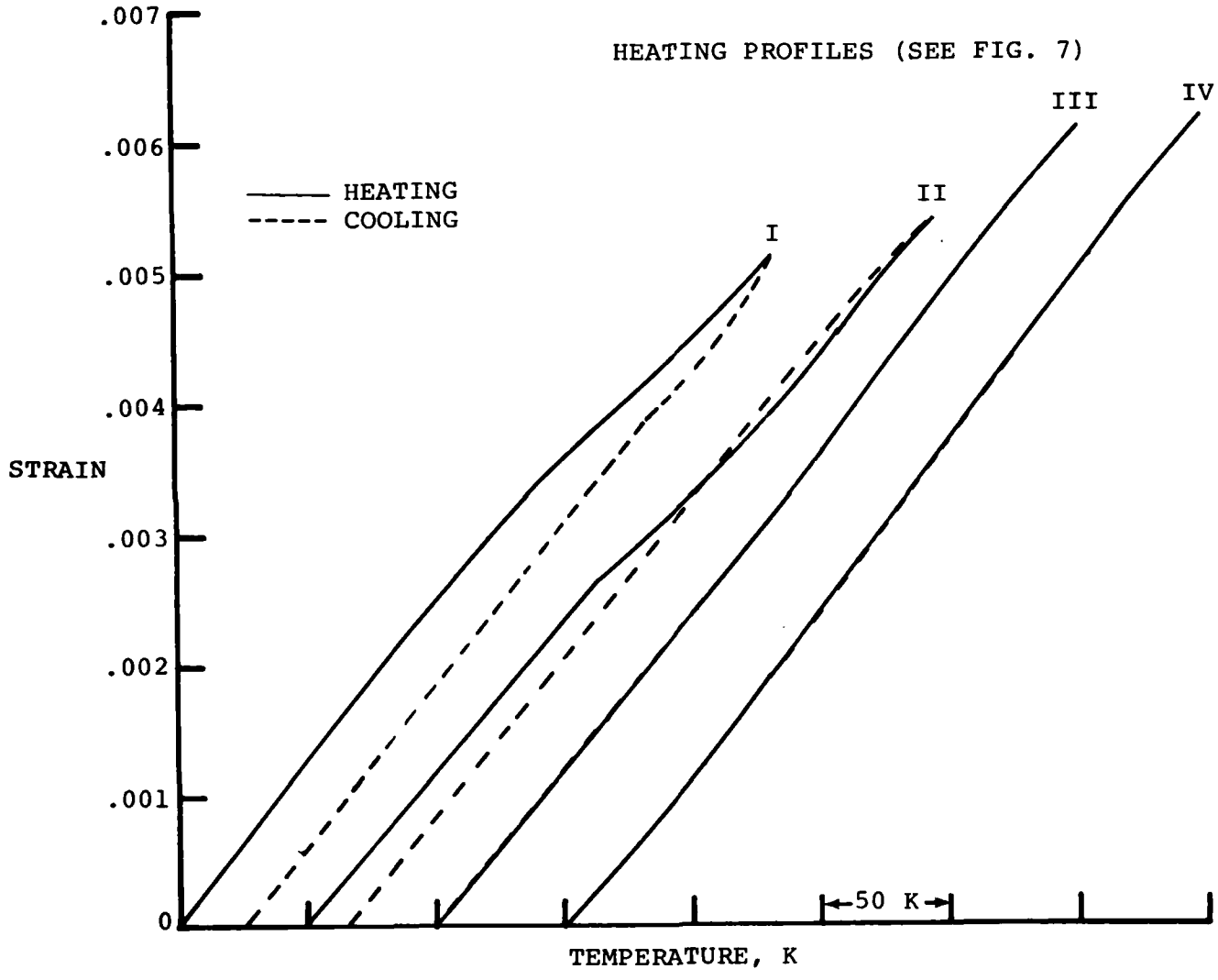

Figure 8.- Effect of heating profiles on longitudinal strain of $[90_4]$ Gr/PI specimen.

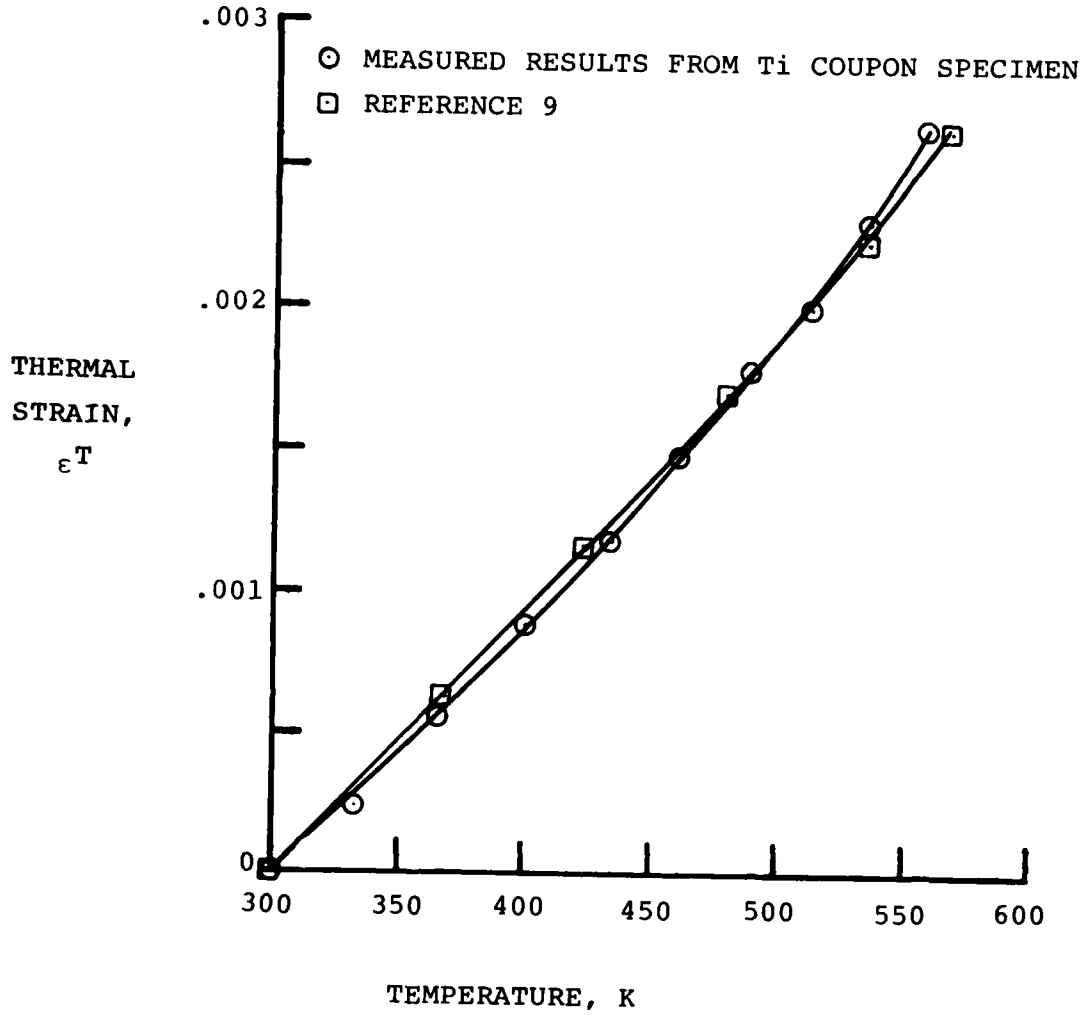

Figure 9.- Comparison of thermal strain measurements of titanium specimen.

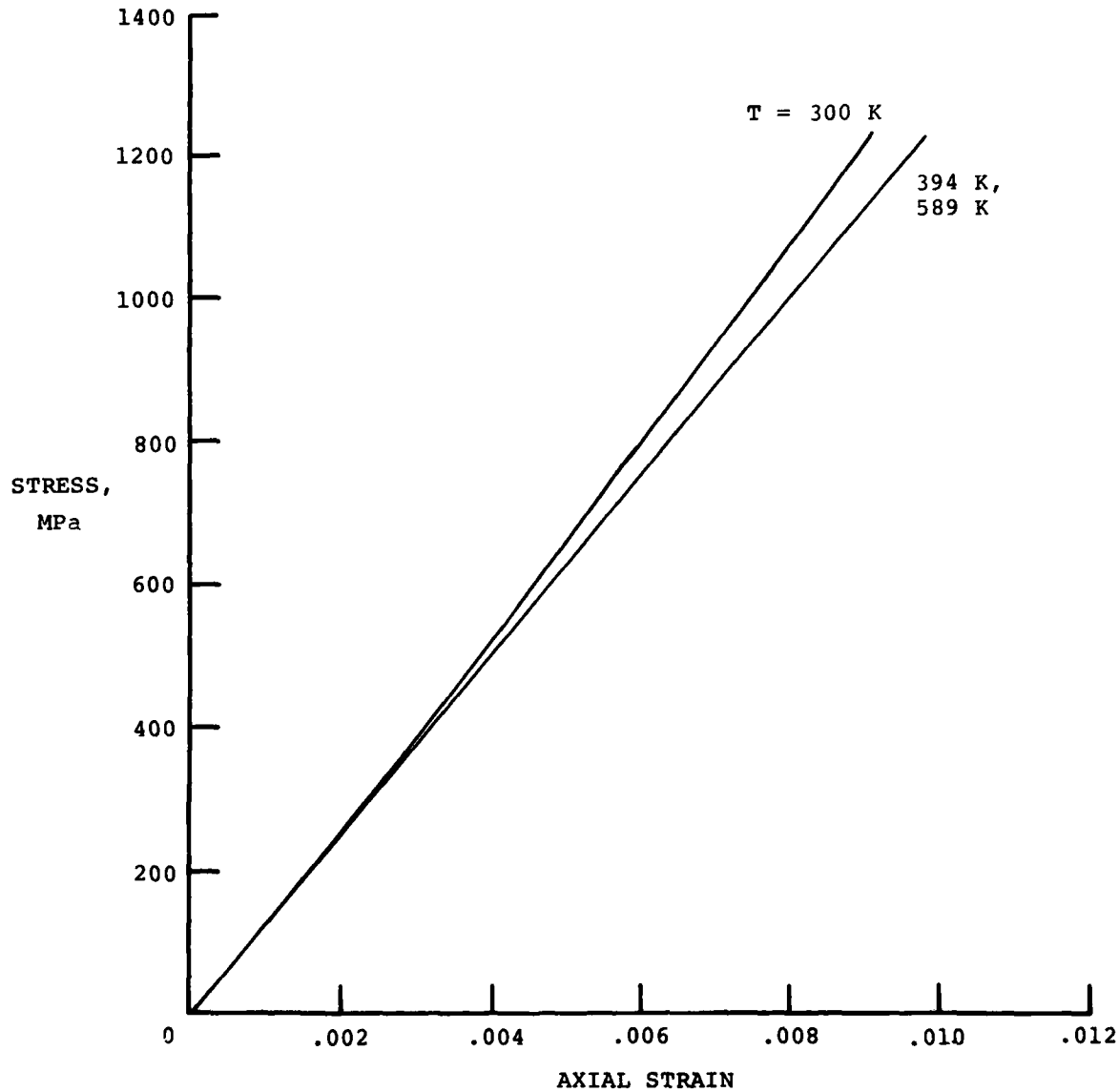

Figure 10.- $[0_4]$ temperature-dependent stress-strain curves of Gr/PI for determining $E_{11}(\sigma,T)$.

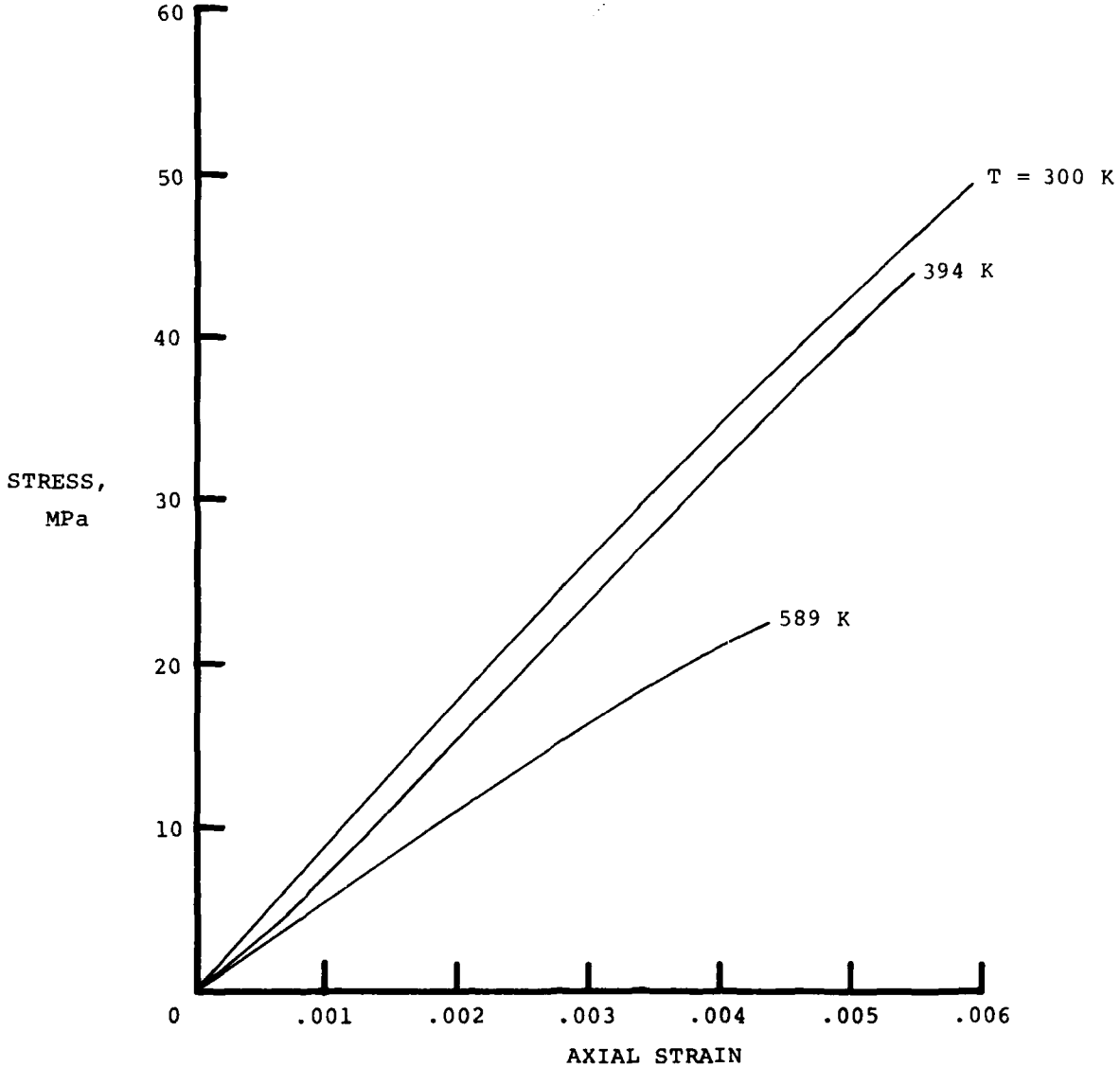

Figure 11.- $[90_4]$ temperature-dependent stress-strain curves of Gr/PI for determining $E_{22}(\sigma,T)$.

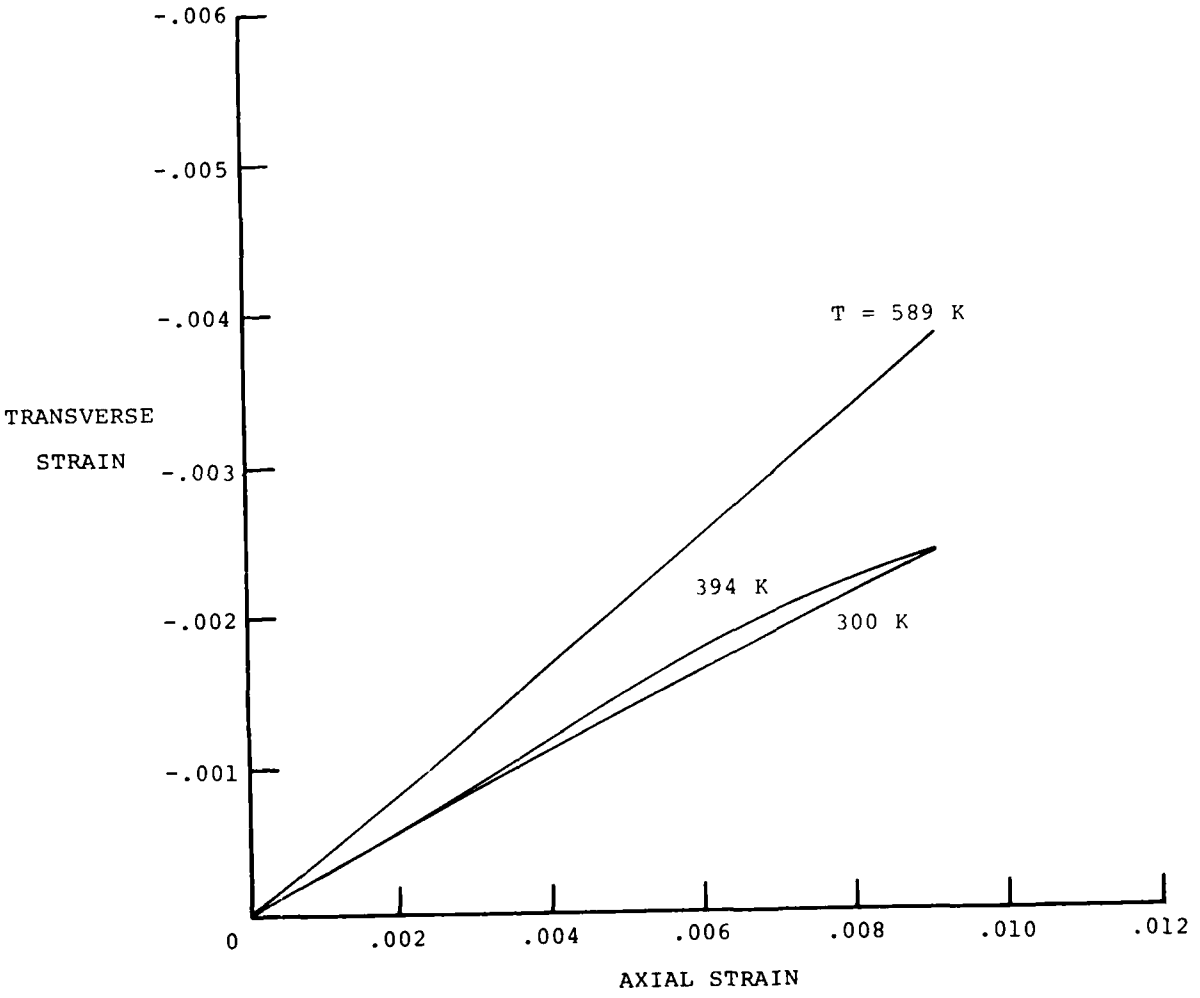

Figure 12.- $[0_4]$ temperature-dependent transverse-axial strain curves of Gr/PI for determining $\nu_{12}(\varepsilon,T)$.

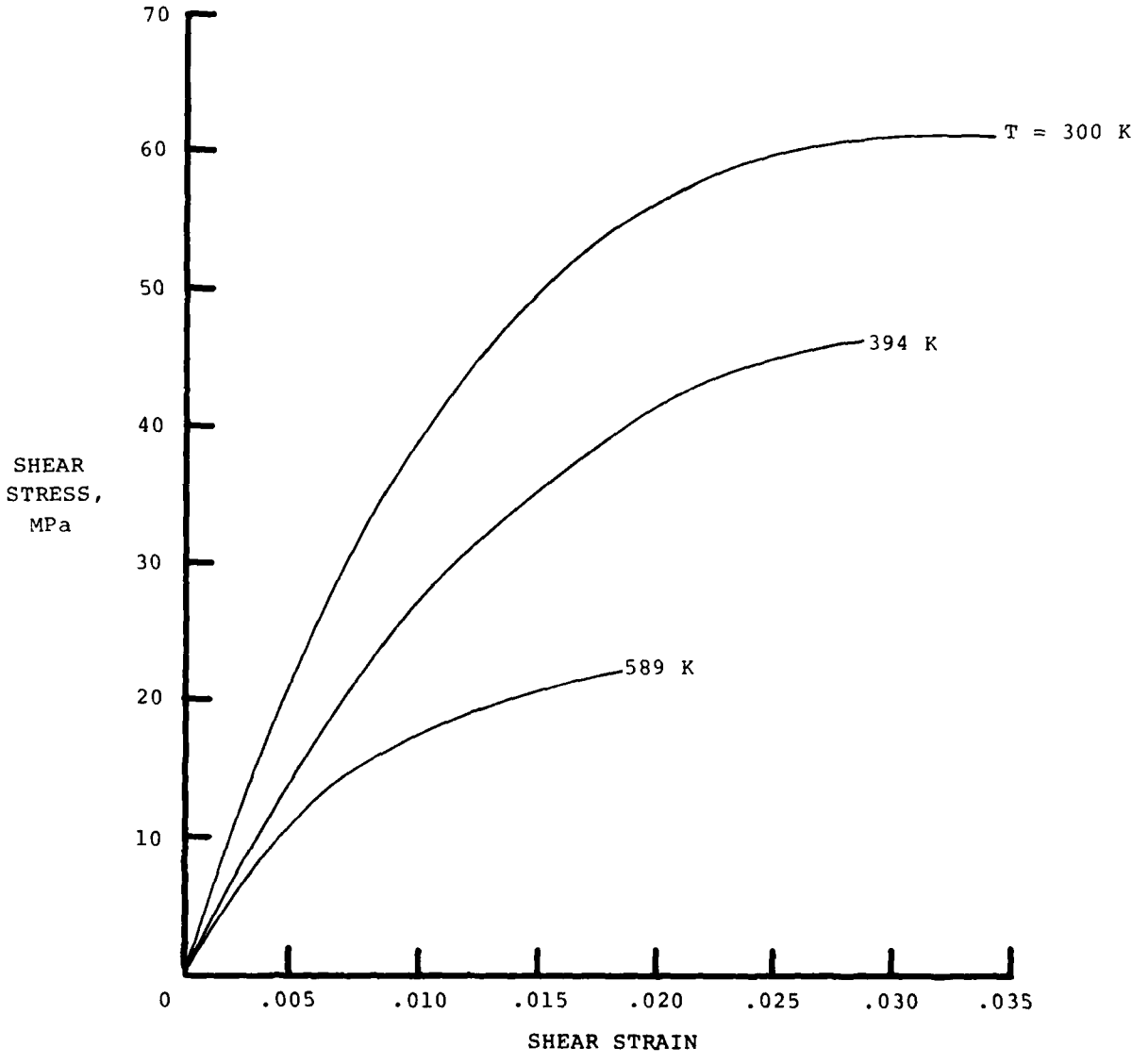

Figure 13.- Temperature-dependent in-plane shear stress-strain response of $[\pm 45]_s$ laminate for determining $G_{12}(\tau,T)$.

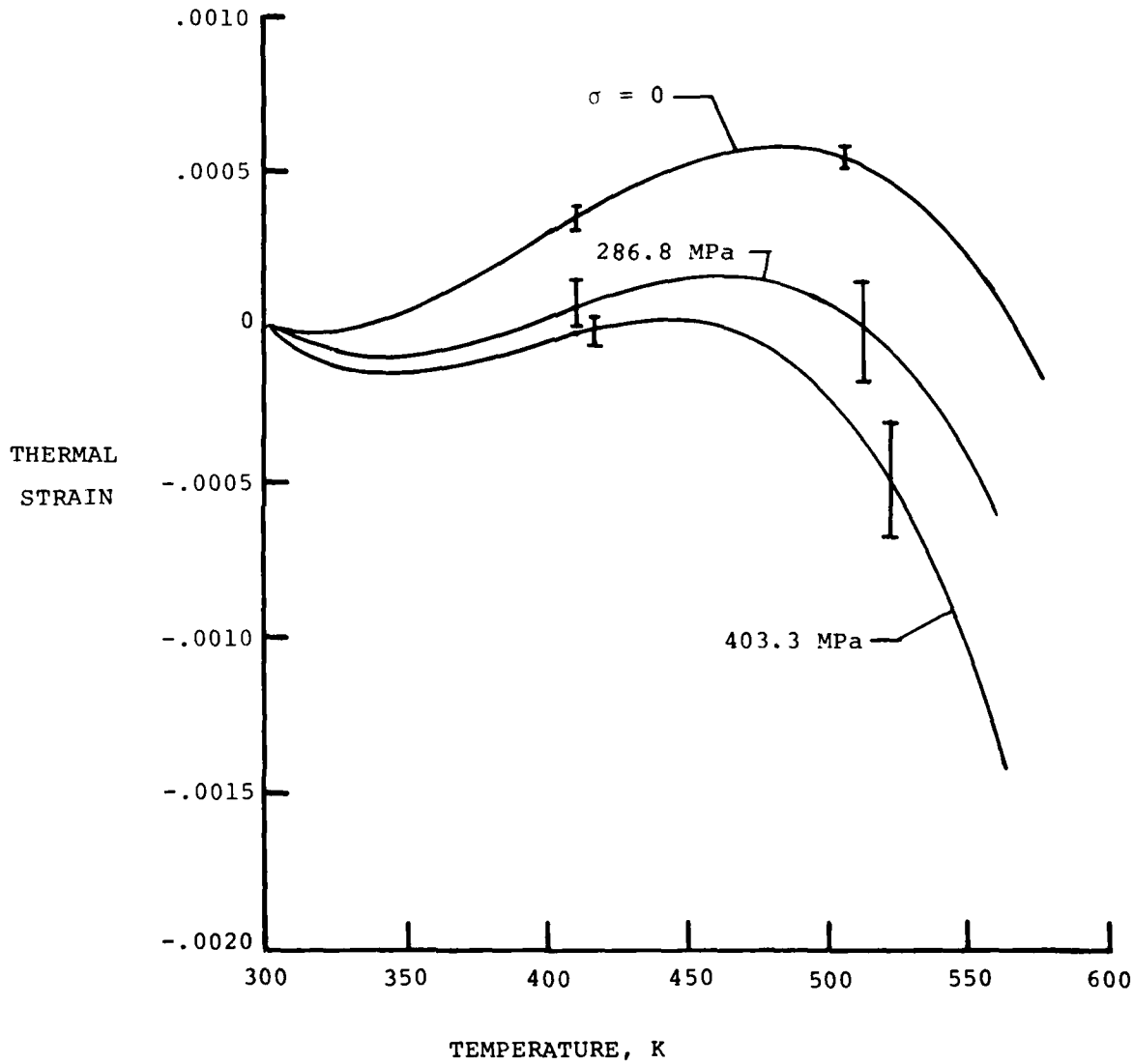

Figure 14.- Measured longitudinal thermal strain of $[0_4]$ Gr/PI laminate as function of temperature and static tensile stress.

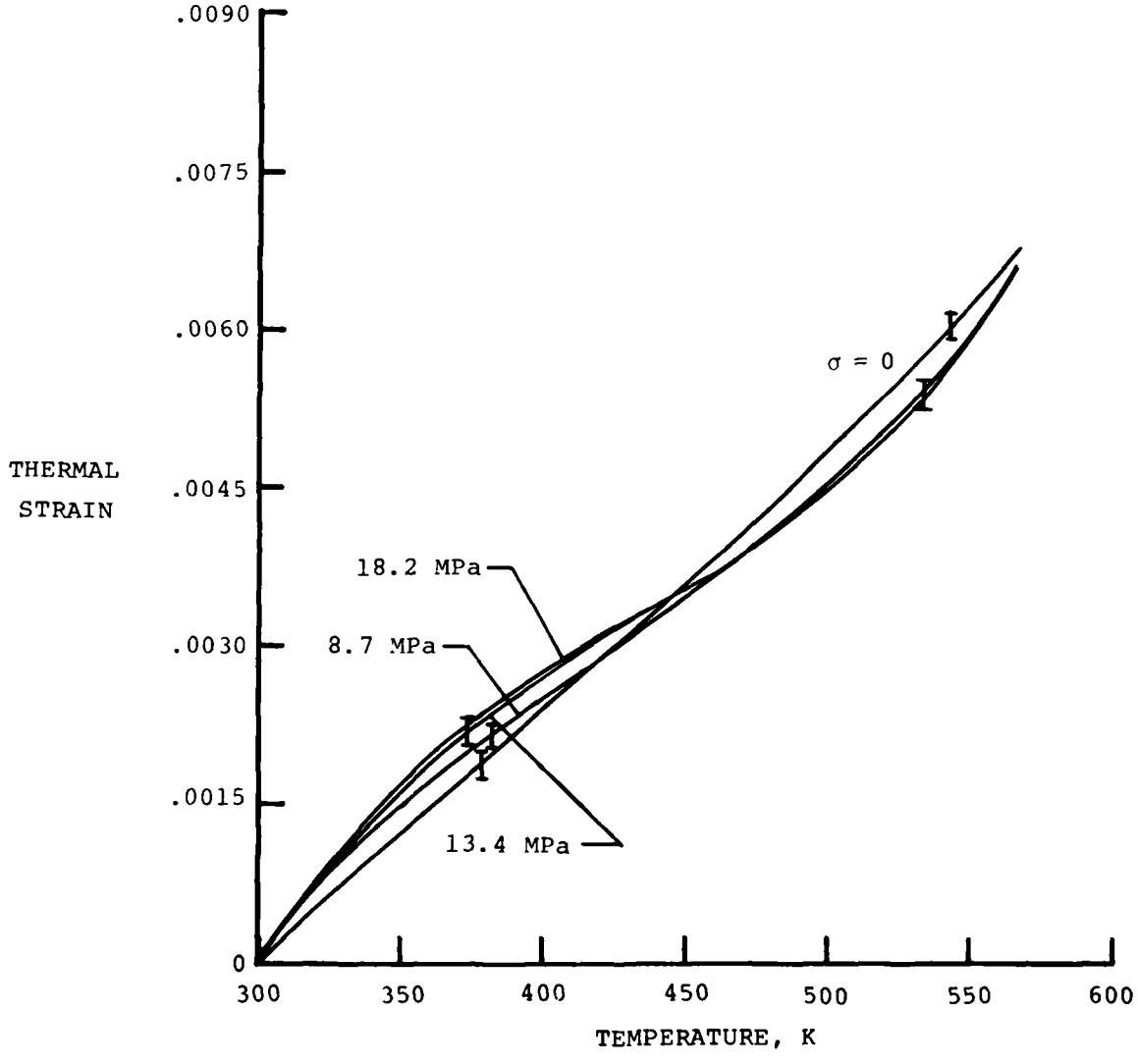

Figure 15.- Measured longitudinal thermal strain of $[90_4]$ Gr/PI laminate as function of temperature and static tensile stress.

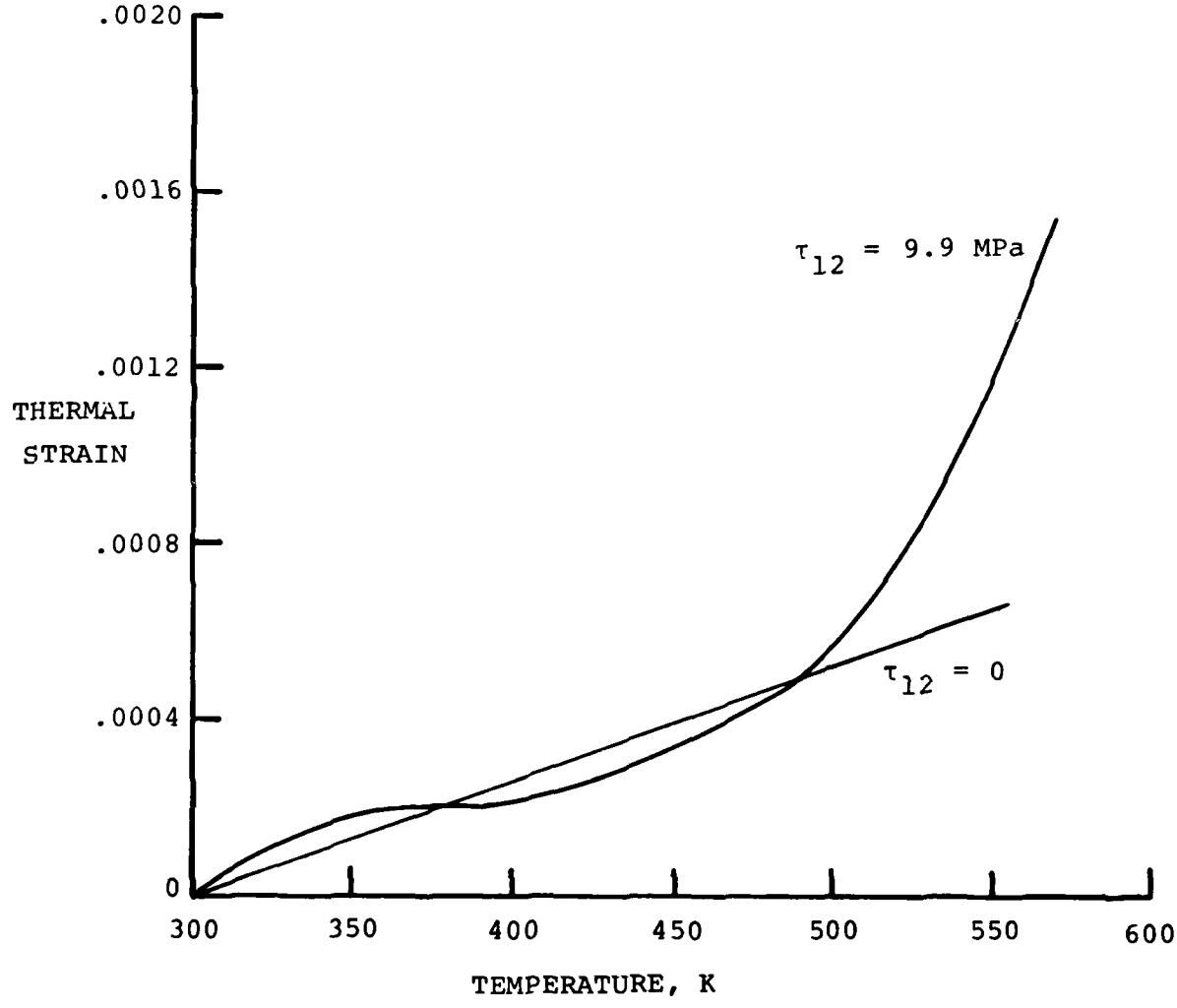

Figure 16.- Thermal strain in fiber direction in $[\pm 45]_s$ laminate as function of temperature and applied static shear stress τ_{12}.

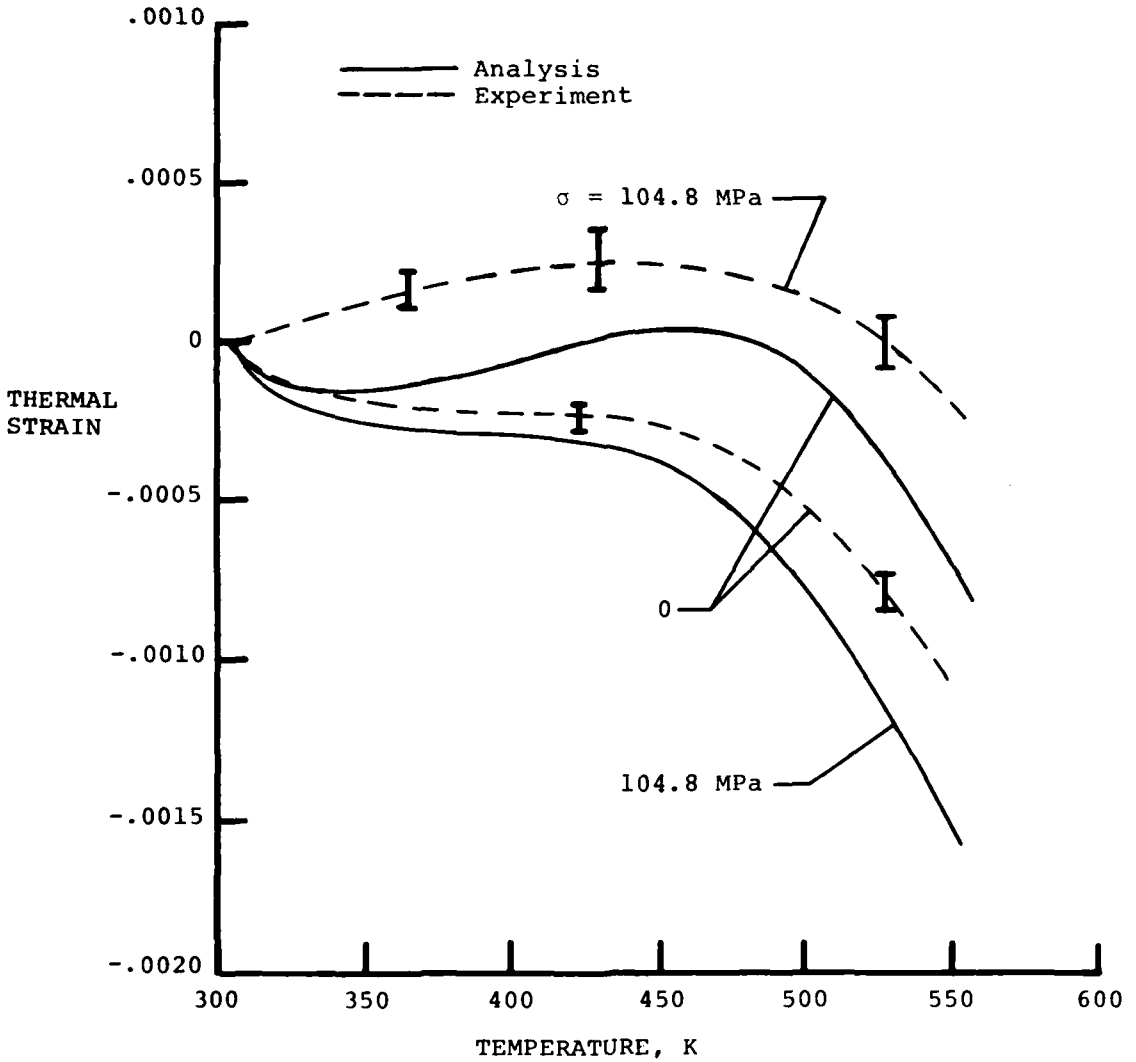

Figure 17.- Measured and calculated longitudinal thermal strain of $[\pm 30]_s$ Gr/PI laminate as function of temperature and static tensile stress.

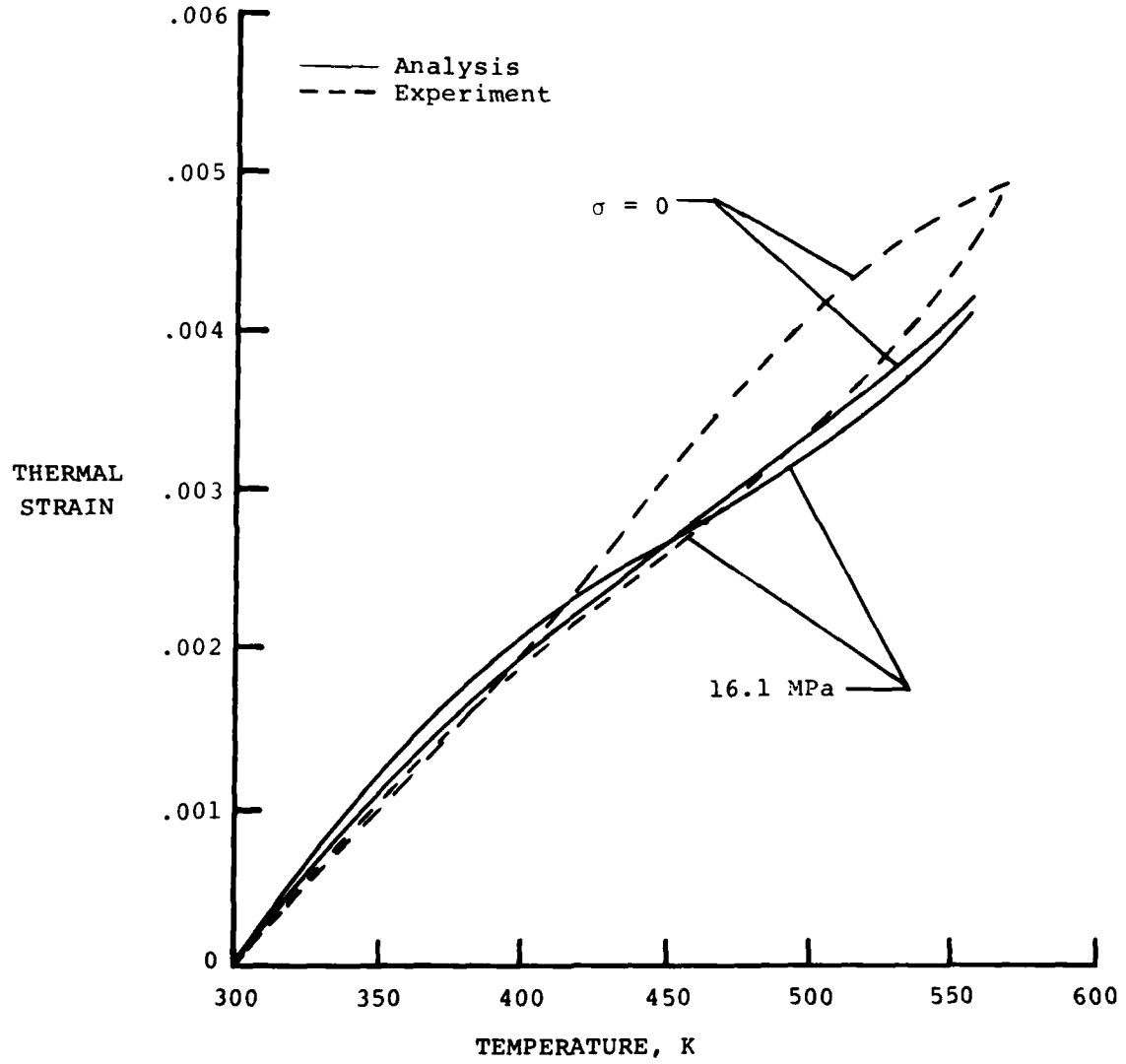

Figure 18.- Measured and calculated longitudinal thermal strain of $[\pm 60]_s$ Gr/PI laminate as function of temperature and static tensile stress.

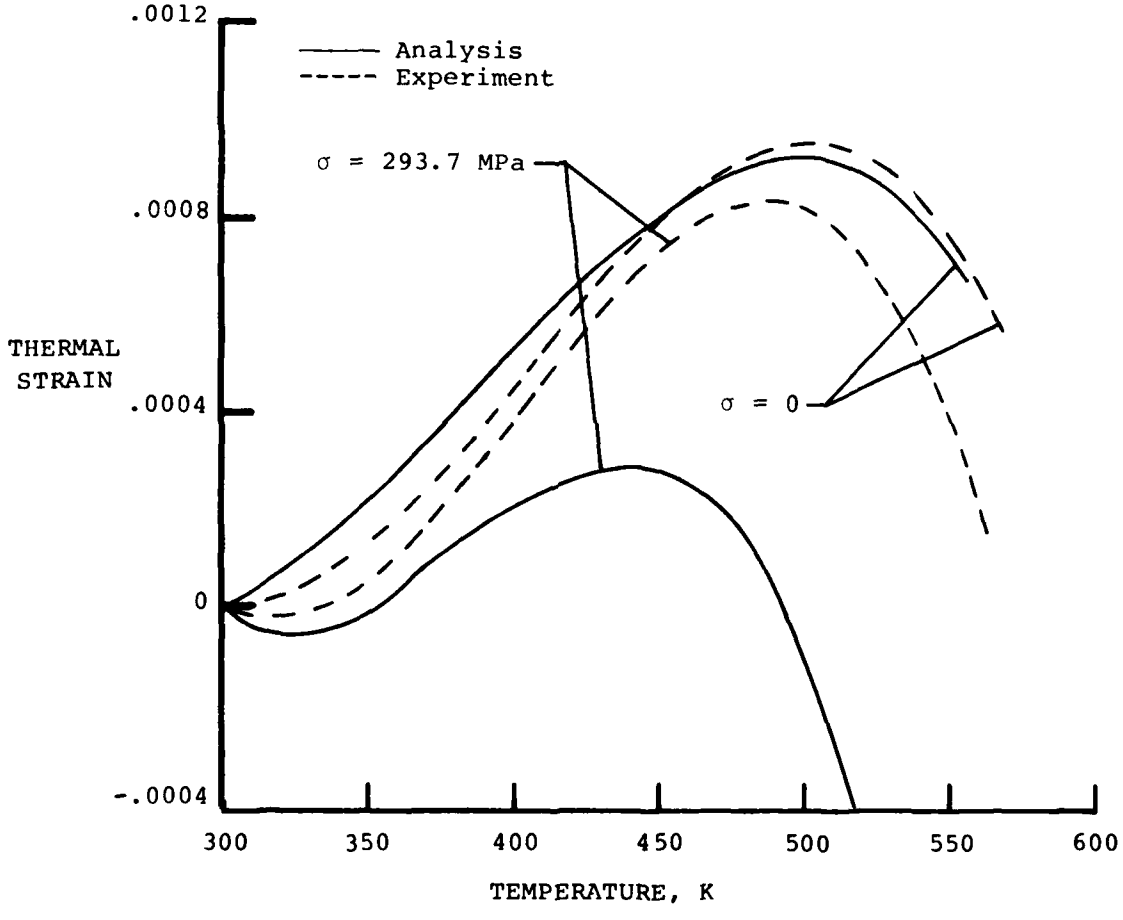

Figure 19.- Measured and calculated longitudinal thermal strain of $[0/90]_s$ Gr/PI laminate as function of temperature and static tensile stress.

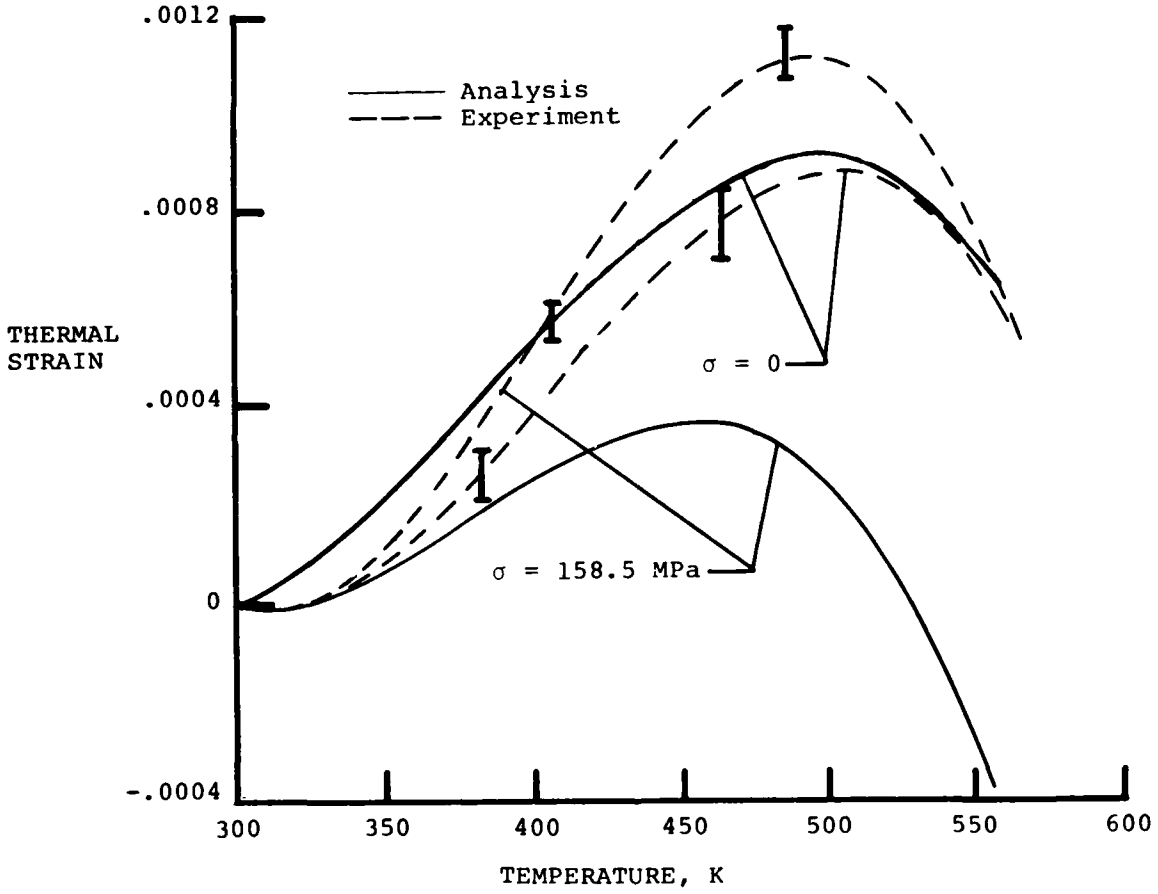

Figure 20.- Measured and calculated longitudinal thermal strain of $[90/-45/0/45]_s$ Gr/PI laminate as function of temperature and static tensile stress.

1 Report No.	2 Government Accession No.	3 Recipient's Catalog No.
NASA TP-1867 AVRADCOM TR 81-B-2	AD-A099805	

4 Title and Subtitle	5 Report Date
EFFECTS OF STATIC TENSILE LOAD ON THE THERMAL EXPANSION OF Gr/PI COMPOSITE MATERIAL	June 1981
	6 Performing Organization Code: 505-33-33-07
7 Author(s): Gary L. Farley	8 Performing Organization Report No.: L-14012
9 Performing Organization Name and Address: Structures Laboratory, AVRADCOM Research and Technology Laboratories, NASA Langley Research Center, Hampton, VA 23665	10 Work Unit No.
	11 Contract or Grant No.
12 Sponsoring Agency Name and Address: National Aeronautics and Space Administration, Washington, DC 20546 and U.S. Army Aviation Research and Development Command, St. Louis, MO 63166	13 Type of Report and Period Covered: Technical Paper
	14 Army Project No.: 1L161102AH45

15 Supplementary Notes

Gary L. Farley: Structures Laboratory, AVRADCOM Research and Technology Laboratories.

16 Abstract

The effect of static tensile load on the thermal expansion of Gr/PI composite material was measured for seven different laminate configurations. A computer program was developed which implements laminate theory in a piecewise linear fashion to predict the coupled nonlinear thermomechanical behavior. Static tensile load significantly affected the thermal expansion characteristics of the laminates tested. This effect is attributed to a fiber-instability micromechanical behavior of the constituent materials. Analytical results correlated reasonably well with free thermal expansion tests (no load applied to the specimen). However, correlation was poor for tests with an applied load.

17 Key Words (Suggested by Author(s))	18 Distribution Statement
Thermal expansion Applied load Graphite polyimide Composite material Stress	Unclassified - Unlimited Subject Category 24

19 Security Classif. (of this report)	20 Security Classif. (of this page)	21 No. of Pages	22 Price*
Unclassified	Unclassified	32	A03

*For sale by the National Technical Information Service, Springfield, Virginia 22161

NASA-Langley, 1981


ATE
LME